Asian Journal of Chemistry; *Vol. 36, No. 6 (2024), 1417-1422*

ASIAN JOURNAL OF CHEMISTRY

https://doi.org/10.14233/ajchem.2024.31559

Novel Carbazoles as AChE Inhibitors: Synthesis, Molecular Docking and Dynamic Simulation Studies

EKTA KHARE[1,2], ZEESHAN FATIMA[1,*], O.P. TIWARI[3], JEEVAN PATRA[1] and UNNATI KUSHAVAH[4]

[1]Amity Institute of Pharmacy Lucknow, Amity University Uttar Pradesh, Sector 125, Noida-201313, India
[2]Department of Pharmaceutical Chemistry, GCRG College of Pharmacy, Lucknow-271835, India
[3]Department of Pharmaceutical Chemistry, Vindhya Gurukul College of Pharmacy (Affiliated to Dr. A. P. J. Abdul Kalam Technical University, Uttar Pradesh), Lucknow-226021, India
[4]Biochemistry and Structural Biology Division, CSIR-Central Drug Research Institute, Sitapur Road, Lucknow-226031, India

*Corresponding author: E-mail: zfatima@amity.edu

Received: 10 March 2024; *Accepted*: 17 May 2024; *Published online*: 31 May 2024; AJC-21657

Extensive exploration of *N*-substituted carbazole derivatives is underway as these compounds possess the therapeutic potential to address the neurological problems. The main aim of this study is to synthesize a series of *N*-substituted carbazole derivatives and investigate it's *in vitro* and *in silico* ability to act as AChE inhibitors. The two-step synthesis was carried out that resulted in the development of novel carbazoles and then these were subsequently subjected to *in vitro* evaluation for acetylcholinesterase (AChE) inhibitory activity. Further to comprehend the binding interactions and establish a plausible binding mechanism, the molecular docking, molecular dynamics and computational ADME predictions were employed. Based on its IC_{50} value of 14.14 μM, -7.327 Kcal/mol binding energy and occupancy of the egg yolk region, which suggests the potential for brain entry, compound **4c** was determined to be an active one among the synthesized compounds. Thus, compound **4c** has the potential to be an AChE inhibitor and effective in treating Alzheimer's disease.

Keywords: Carbazoles, Acetylcholinesterase inhibitors, Anti-Alzheimer, Synthesis, Molecular docking, Dynamics.

INTRODUCTION

Alzheimer's disease is a chronic and progressive neurodegenerative disorder characterized by memory loss, cognitive dysfunction and behavioural abnormalities [1]. Globally, over 50 million individuals are affected by Alzheimer's disease, a number expected to surge to 13.8 million by 2060 [2,3]. The pathogenesis of Alzheimer's disease is complex and multifactorial, with several contributing factors still not fully understood [4]. The most significant factor is the deficit of acetylcholine, a neurotransmitter crucial for memory and learning [5]. Several clinical acetylcholinestrase drugs approved by the US FDA such as donepezil, rivastigmine and galantamine are the main drugs for Alzheimer's disease management [6]. The reliability of these clinical candidates weakened due to their various adverse effects such as hypotension and hepatotoxicity [7]. Despite of their adverse effects, acetylcholinesterase drug target is a valuable strategy for exploring novel chemotypes for Alzheimer's disease management. Over a decade several studies shown that acetylcholinesterase served as a multifactorial tool with the other key targets such as butyrylcholinesterase (BuChE), monoamine oxidase B (MAO-B), amyloid-β (Aβ) and β-secretase-1 (BACE1) [8,9].

Carbazole proven as an important bioactive scaffold having wide range of biological activities [10-14]. The carbazole [15-17] and carbamates [18-21] derivatives demonstrated promising biological activities against Alzheimer's disease by targeting multiple pathological pathways. The carbamate is the core scaffold of the FDA approved drug rivastigmine. According to the AChE crystallographic research, a deep canyon groove is found in the catalytic active site (CAS), including Ser-His-Glu, and at the entrance of the canyon, peripheral anionic site (PAS) [22,23]. For the Alzheimer's disease management, the designed inhibitors must interact with both CAS and PAS residues [24, 25]. Inspiring from the available anti-Alzheimer's disease clinical candidates and potent literature source, we developed a novel multifunctional pharmacophore where carbazole is fused with carbamate scaffold to explore its efficacy against multiple

Alzheimer's disease targets. The designed rationale hybrids don't have any CNS drug filter violation and possess optimum pharmacokinetic profile as like anti-Alzheimer's disease clinical drugs. Several reports suggested that the presence of substituted phenyl ring projecting towards the entrance cavity of AChE [26]. Hence, various substitutions at *para* position on the phenyl ring [27] is performed. This forms the crucial π-π interactions with active aromatic residues, enhance BBB permeability and potency [28]. In this study, we synthesized designed hybrids, evaluated its biological potency against AChE and finally corroborated its inhibition activity based on the molecular modelling using MM-GBSA and NBE energies and dynamics for the protein-ligand stability.

EXPERIMENTAL

All chemicals, including starting materials, reagents and solvents, were purchased from commercial suppliers such as Sigma-Aldrich and Merck, USA. Column chromatography using Merck silica gel (70-230 mesh) was used for the purification of intermediates and final products. FTIR spectra were recorded on a Shimadzu 8400 S spectrophotometer using KBr discs. Mass spectra were recorded using a water OPLC-TQDMS on a positive-mode ESI-MS spectrophotometer and ^{1}H NMR spectra were recorded on a JEOL AL 300 MHz spectrometer using TMS as an internal standard in DMSO/$CDCl_3$.

Synthesis of *N*-substituted carbazoles: In the first step, intermediate 6-hydroxy-pyridocarbazol-4-one (**3**) was carried out according to the reported method [29]. The procedure includes condensation of carbazole with malonic acid in presence of phosphoryl chloride. The reaction was carried out at 120 ºC for 4-5 h and the product obtained was further utilized to sythe-size the titled compounds.

In second step, the synthesized intermediate 6-hydroxy-pyridocarbazol-4-one (**3**) was condensed with isocyanate derivatives in the presence of dry THF and NaH (0.24 g) in equimolar qantities at 10 ºC and then the reaction mixture was stirred for 4-5 h. Ethyl acetate and hexane was used to develope the TLC which was visualized under iodine to monitor the progress of the reaction. The product so obtained was filtered, washed and recrystallized with absolute ethanol (**Scheme-I**). The melting point of the compounds were recorded and all the compounds were characteized by IR, ^{1}H NMR and high resolution MASS spectrometry.

6-Hydroxy-4*H*-pyridocarbazol-4-one (3): Creamy white colour; yield: 65%; m.p. 310-312 ºC; ^{1}H NMR (500 MHz, DMSO, δ ppm): 12.1 (s, 1H) OH, 7.5-8.5 (m, 7H) CH aromatic, 6.0 (s, 1H) CH.

4-Oxo-4*H*-pyridocarbazol-6-yl-4-nitrophenylcarbamate (4a): Reddish colour; yield: 55%; m.p. 314-316 ºC; Anal. Calcd. (found) % for $C_{22}H_{13}N_3O_5$: C, 66.17 (66.15); H, 3.28 (3.29); N, 10.52 (10.50); O, 20.03 (20.05). IR (KBr, ν_{max}, cm^{-1}): 3235 (NH), 1739 (C=O ester *str.*), 1550 (C-NO_2), 1300 (C-O ester *str.*), 847 (*para*-position); ^{1}H NMR (500 MHz, DMSO, δ ppm): 9.8 (s, 1H) NH, 6.5-8.5 (m, 11H) CH aromatic, 5.9 (s, 1H) CH; ESI-MS calcd. for $C_{22}H_{13}N_3O_5$: *m/z* (M-H, 100) = 398.

4-Oxo-4*H*-pyridocarbazol-6-yl *p*-chloro carbamate (4b): White coloured powder, yield: 65%; m.p. 318-320 ºC; Anal. calcd. (found) % for $C_{22}H_{13}ClN_2O_3$: C, 67.96 (67.97); H, 3.37 (3.34); Cl, 9.12 (9.13); N, 7.21(7.23); O, 12.35 (12.36). IR (KBr, ν_{max}, cm^{-1}): 3296 (NH), 1772 (C=O ester *str.*), 1236 (C-O ester *str.*), 823 (*para* position), 717 (C-Cl); ^{1}H NMR (500 MHz, DMSO, δ ppm): 9.2 (s, 1H) NH, 7.4-8.6 (m, 11H) CH aromatic, 6.0 (s, 1H) CH; ESI-MS calcd. for $C_{22}H_{13}ClN_2O_3$: *m/z* (M-1, 100) = 387.

4-Oxo-4*H*-pyridocarbazol-6-yl *p*-fluro-carbamate (4c): Yellowish white, yield: 50%; m.p. 300-302 ºC; Anal. calcd. (found) % for $C_{22}H_{13}FN_2O_3$: C, 70.96 (70.95); H, 3.52(3.50); F, 5.10 (5.13); N, 7.52 (7.53); O, 12.89 (12.87). IR (KBr, ν_{max}, cm^{-1}): 3294 (NH), 1632 (C=O ester *str.*), 1347 (C-F *str.*), 1209 (C-O ester *str.*), 831 (*para* position); ^{1}H NMR (500 MHz, DMSO, δ ppm): 9.2 (s, 1H) NH, 6.8-8.6 (m, 11H) CH aromatic, 6.0 (s, 1H) CH; ESI-MS calcd. for $C_{22}H_{13}FN_2O_3$: *m/z* (M-1, 100) = 371.

4-Oxo-4*H*-pyridocarbazol-6-yl-*p*-methyl carbamate (4d): White coloured powder, yield: 56%; m.p. 320-322 ºC; Anal. calcd. (found) % for $C_{23}H_{16}N_2O_3$: C, 74.99 (74.95); H, 4.38 (4.41); N, 7.60 (7.58); O, 13.03 (13.06). IR (KBr, ν_{max}, cm^{-1}): 3314 (NH), 2758 (C-CH_3), 1702 (C=O ester *str.*), 1303 (C-O ester *str.*), 830 (*para* position); ^{1}H NMR (500 MHz, DMSO, δ ppm): 8.9 (s, 1H) NH, 7.4-8.5 (m, 11H) CH aromatic, 6.0 (s, 1H) CH, 2.2 (s, 3H) methyl; ESI-MS calcd. for $C_{23}H_{16}N_2O_3$: *m/z* (M-1, 100) = 367.

4-Oxo-4*H*-pyrido-carbazol-6-yl *p*-methoxy carbamate (4e): Reddish white colour, yield: 55%; m.p. 318-320 ºC; Anal. calcd. (found) % for $C_{23}H_{16}N_2O_4$: C, 71.87 (71.84); H, 4.20 (4.22); N, 7.29 (7.27); O, 16.65 (16.68). IR (KBr, ν_{max}, cm^{-1}):

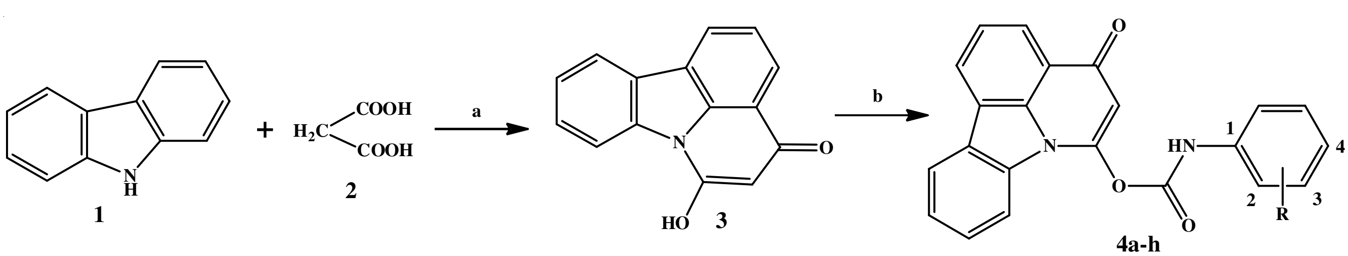

Scheme-I: Synthetic strategy for titled compounds **4a-h**; Reagents & conditions: (a) $POCl_3$ at 70-80 °C, (b) Substituted isocyanates, NaH, dry THF at 10 °C

3320 (NH), 1700 (C=O ester *str.*), 1232 (C-O ester *str.*), 826 (*para*-position) ^{1}H NMR (500 MHz, DMSO, δ ppm): 8.8 (s, 1H) NH, 6.8-8.4 (m, 11H) CH aromatic, 6.0 (s, 1H) CH, 3.9 (s, 3 H) methoxy; ESI-MS calcd. for $C_{23}H_{16}N_2O_4$: *m/z* (M-1, 100) = 383.

4-Oxo-4*H*-pyrido-carbazol-6-yl-2,4-dichlorophenylcarbamate (4f): White colour solid, yield: 66%; m.p. 314-316 ºC; Anal. calcd. (found) % for $C_{22}H_{12}Cl_2N_2O_3$: C, 62.43 (62.44); H, 2.86 (2.84); Cl, 16.75 (16.73); N, 6.62 (6.65); O, 11.34 (11.34). IR (KBr, ν_{max}, cm^{-1}): 3297 (NH), 1632 (C=O ester *str.*), 1290 (C-O ester *str.*), 828 (*para* position), 558 & 625 (C-Cl *str.*); ^{1}H NMR (500 MHz, DMSO, δ ppm): 9.2 (s, 1H) NH, 6.8 -8.5 (m, 10H) CH aromatic, 6.2 (s, 1H) CH; ESI-MS calcd. for $C_{22}H_{12}Cl_2N_2O_3$: *m/z* (m-H, 100) = 422.

4-Oxo-4*H*-pyrido-carbazol-6-yl-3-nitrophenylcarbamate (4g): Creamy white, yield: 60%, m.p. 315-317 ºC; Anal. calcd. (found) % for $C_{22}H_{13}N_3O_5$: C, 66.17 (66.14); H, 3.28 (3.26); N, 10.52 (10.51); O, 20.03(20.08). IR (KBr, ν_{max}, cm^{-1}): 3346 (NH), 1707 (C=O ester *str.*), 1526 (C-NO_2), 1239 (C-O ester *str.*), 735 (*meta*-position); ^{1}H NMR (500 MHz, DMSO, δ ppm): 9.5 (s, 1H) NH, 6.8-8.5 (m, 11H) CH aromatic, 6.2 (s, 1H) CH; ESI-MS calcd. for $C_{22}H_{13}N_3O_5$: *m/z* (M-H, 100) = 398

4-Oxo-4*H*-pyrido-carbazol-6-yl-3-chlorophenylcarbamate (4h): Creamish white, yield: 66%; m.p. 315-317 ºC; Anal. calcd. (found) % for $C_{22}H_{13}ClN_2O_3$: C, 67.96 (67.94); H, 3.37 (3.36); Cl, 9.12 (9.11); N, 7.21 (7.22); O, 12.35 (12.37). IR (KBr, ν_{max}, cm^{-1}): 3293 (NH), 1711 (C=O ester *str.*), 1285 (C-O ester *str.*), 726 (*m*-chloro), 641 (C-Cl *str.*); ^{1}H NMR (500 MHz, DMSO, δ ppm): 8.5 (s, 1H) NH, 6.8-8.3 (m, 11H) CH aromatic, 6.86 (s, 1H) CH; ESI-MS calcd. for $C_{22}H_{13}ClN_2O_3$: *m/z* (m-H, 100) = 387

Molecular docking and dynamics: The molecular docking studies was performed by using Glide docking program, Schrödinger Maestro software (version 11.1.012; Schrodinger LLC, New York), at CDRI, Lucknow. All the synthesized ligands were designed, prepared and protonated with Epik at pH 7.4 ± 0.2 using LigPrep. The obtained crystallographic structure of AChE (PDB ID: 1GQR) was retrieved from the RCSB PDB bank [30]. The receptor grid centroid was defined at the rivastigmine bounded site. The binding modes of the estimated by the xtra precision glide docking and MMGBSA using Prime. The inter-action networks were visualized with PyMOL and BIOVIA discovery studio.

Molecular dynamics simulation studies were performed using Desmond 2023-1 software. The systems were enclosed in an orthorhombic solvation box with a 10 Å absolute buffer size and was solvated using TIP5P (transferable intermolecular potential with 5 points) model. The simulation systems were neutralized with counter Na^+ ions and a 0.15 M salt concentration was applied. Minimization was performed using the steepest descent algorithm and conjugate gradient for 2000 steps and 3000 steps, respectively. The system was maintained isotopically by the Martyna Tobias Klein barostat and Noose Hoover thermostat at 1.013 bar and 300 K, respectively. Simulations were performed for up to 50 ns using the OPLS4 force field.

Physico-chemical and pharmacokinetic assessment: The Swiss ADME software web tool http://www.swissadme.ch was accessed to estimate individual ADME characteristics of the synthesized compounds. The compounds were sketched on the server provided space and were converted to Simplified Molecular Input Line Entry System string (SMILES) thereafter the result was obtained in tabular format. The drug-like properties, pharmacokinetic and physico-chemical properties of the compounds were studied. Besides this Brain Or IntestinaL EstimateD permeation method (BOILED EGG) was used to predict the permeation of designed molecule [31,32].

Biological evaluation: *In vitro* AChE inhibitory activity was conducted as per the standard procedure of Ellman's method with minor modifications [33]. A 40 mL of the test solution in various concentrations was taken with 50 mL of 50 mM Tris-HCl buffer (pH 8.0) and 50 mL of 0.02 U/mL AChE. Initially, the solution was pre-incubated for 30 min at 4 ºC. The reaction mixture was then supplemented with 30 mL of 10 mM DTNB (5,5′-dithiobis-2-nitrobenzoic acid) and 30 mL of 12 mM ATChI (acetylthiocholine iodide). During a 10 min interval at 25 ºC, AChE activity was detected using an Elisa reader. By comparing the enzyme's activity with and without the inhibitor, the percentage of inhibition was determined comparing the enzyme activity with and without inhibitor. Rivastigmine was used as positive control and the experimental values were taken in triplicates.

RESULTS AND DISCUSSION

Structure activity relationship (SAR) studies: It has been found that halogens are more effective than electron withdrawing groups in the phenyl ring, which is significant for pharmacological activity. Best in the inhibition was achieved by compound **4c**, which could be because of the flourine's strong electronegativity and smallest size, which shows IC_{50} value of 14.14 μM. similarly, chlorine present at the *para* position, was found to be 17.52 μM IC_{50} value. Changing the position of chlorine from *para* to *meta*-leads to decrease in the activity *i.e.* compound **4h**. Disubstituted chlorine compound **4f** having -Cl at *ortho* and *para* position further lead to a decrease in the IC_{50} value which was 26.40 μM. However, electron withdrawing substituent nitro, present at the *para* and *meta* position showed low inhibitory activity having IC_{50} value of 31.88 and 34.68 μM, respectively. The electron-withdrawing substituents in compounds **4d** and **4e** at the *para* position also showed low inhibitory activity having an IC_{50}value of 31.30 and 28.05 μM, respectively. All the compounds were found to be relatively less potent as AChE inhibitors (Table-1) when compared to standard drug rivastigmine. Among the electron-donating substituents *viz.* methoxy and methyl group activity were almost alike but it was less than the electron-withdrawing substituents [34].

Molecular modelling interactions: The xtra precision docking revealed similar geometry for all designed analogues inside the active binding pocket. This can be correlated based on the interacting residues (Table-2). Among the designed series, **4c** showed the highest binding affinity, which is confirmed with its inhibition activity against AChE (Table-1). Non-bonded energies (NBEs) are the cumulative energy between van der Waals, electrostatic and coulombic energies. The interacting

TABLE-1
BINDING FREE ENERGIES AND AChE INHIBITION ACTIVITY OF SYNTHESIZED MOLECULES

Compd. No.	R	AChE IC_{50} (µM)	Gscore (kcal/mol)
4a	4-Nitro	31.88 ± 0.41	-7.076
4b	4-Chloro	17.52 ± 0.29	-6.494
4c	4-Fluoro	14.14 ± 0.35	-7.327
4d	4-Methyl	31.30 ± 0.34	-5.995
4e	4-Methoxy	28.05 ± 0.40	-6.955
4f	2,4-Dichloro	26.40 ± 0.55	-8.197
4g	3-Nitro	34.68 ± 0.33	-6.837
4h	3-Chloro	24.15 ± 0.35	-7.232
Rivastigmine	–	11.82 ± 0.35	-7.374

residues of **4c** exhibited identical residues (Fig. 1) as the control group (rivastigmine). Compound **4c** formed aromatic hydrogen bonding, π-π stacking and hydrophobic contacts. The 4-fluoro phenyl group showed aromatic interactions with Phe331 and Tyr334, while the pyrido-carbazole scaffold participated in π-π stacking with Trp84, Phe330 and Tyr121. However, the carbonyl group of the pyridocarbazole scaffold exhibited unfavourable interactions with the His440 residue, possibly due to the torsion hindrance between Gly441 and His440. The per residue energy decomposition showed good residual binding affinities for D72 (-55.57), W84 (-56.21), Y121 (-48.89), F330 (-29.45), F331 (-32.91), Y334 (-45.32) and H440 (-31.40). The molecular dynamics simulations further validated the structural binding phenomena of the best-docked conformer. The AChE-**4c** complex showed consistent binding behaviour (Fig. 2) and maintained the interaction strength throughout the simulation. Specifically, hydrophobic interactions formed with Trp84, Tyr121, Phe290, Phe330, Phe331 and Tyr334 and hydrogen bonding occurred with Glu199 and His440 (Figs. 3 and 4). These interactions resulted in strong binding strength during the simulation course (Fig. 5).

ADME profile: The results support the drug-likeness properties of **4c**, with no violation to Lipinski filter. Also, the radar plot (Fig. 6a) supports the same. The boiled egg model (Fig. 6b) suggests that the molecule is able to penetrate the blood brain barrier as it lies in the yolk region of the model, which is an essential requisite for the molecule to treat neurological disorders.

Conclusion

The study involved the synthesis of eight new carbazole-carbamate hybrid analogs with the aim of exploring their potential as inhibitors of acetylcholinesterase (AChE) for the treatment of Alzheimer's disease. The synthesized compounds showed better activity and among them, the IC_{50} value of compound **4c** was found to be 14.14 µM. The compounds also showed better binding energy which was comparable to that of rivastigmine. Molecular dynamics simulations further substantiated the struc-

TABLE-2
MMGBSA, NBE AND INTERACTING RESIDUES OF SYNTHESIZED MOLECULES

Compd. No.	ΔG	ΔG_{Coul}	ΔG_{lipo}	ΔG_{vdW}	Interacting residues
4a	-39.81	-9.02	-27.92	-65.49	Y334, F330, W84, E199, G117, D72
4b	-36.87	-11.43	-26.53	-55.26	Y334, F330, W84, D72, F331
4c	-44.06	-21.41	-28.00	-53.44	D72, W84, Y121, F330, F331, Y334, H440
4d	-24.88	-9.20	-16.39	-61.86	Y334, F330, W84, E199, G117, D72
4e	-38.83	-11.58	-23.96	-44.41	W84, Y121, W279, F330, F331
4f	-40.63	-11.50	-29.24	-52.46	E199, F330, Y334, F331, D72, W84
4g	-41.73	-8.04	-30.05	-56.50	Y70, Y121, I287, F330, F331
4h	-34.88	-8.30	-21.87	-45.90	D72, W84, Y121, F330, F331, Y334
Rivastigmine	-47.54	-31.51	-28.69	-54.41	D72, W84, Y121, F330, F331, Y334

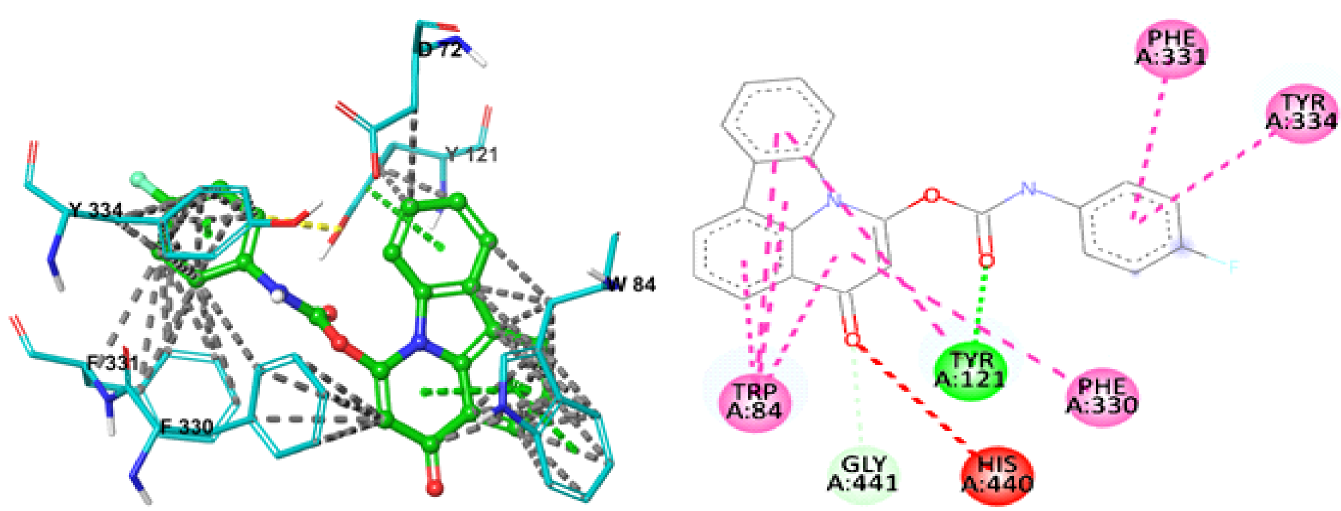

Fig. 1. Molecular interactions of **4c**: hydrophobic, aromatic hydrogen bonding, π-π stacking interactions are represented by grey, magenta, yellow and green dashed lines respectively

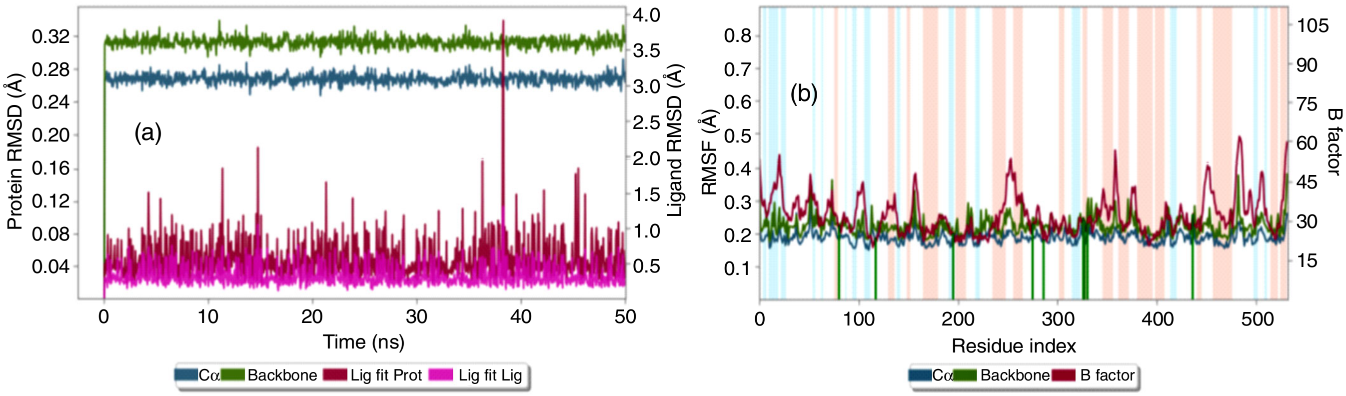

Fig. 2. (a) RMSD and (b) RMSF of AChE-**4c**

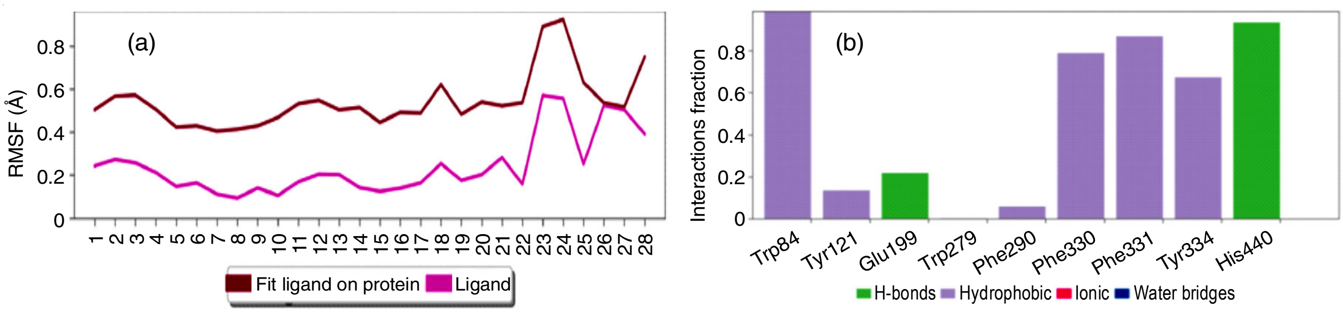

Fig. 3. (a) Ligand **4c** RMSF and (b) Interactions formed during the simulation represented in interaction fractions

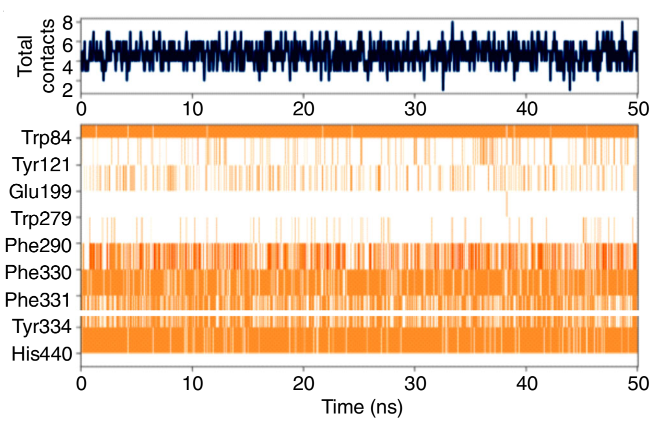

Fig. 4. Heat map showing number of interactions formed during the simulation course

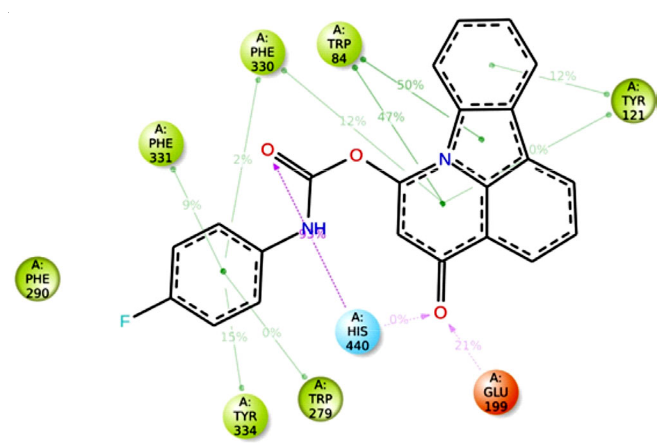

Fig. 5. Interaction strength formed during the simulation course

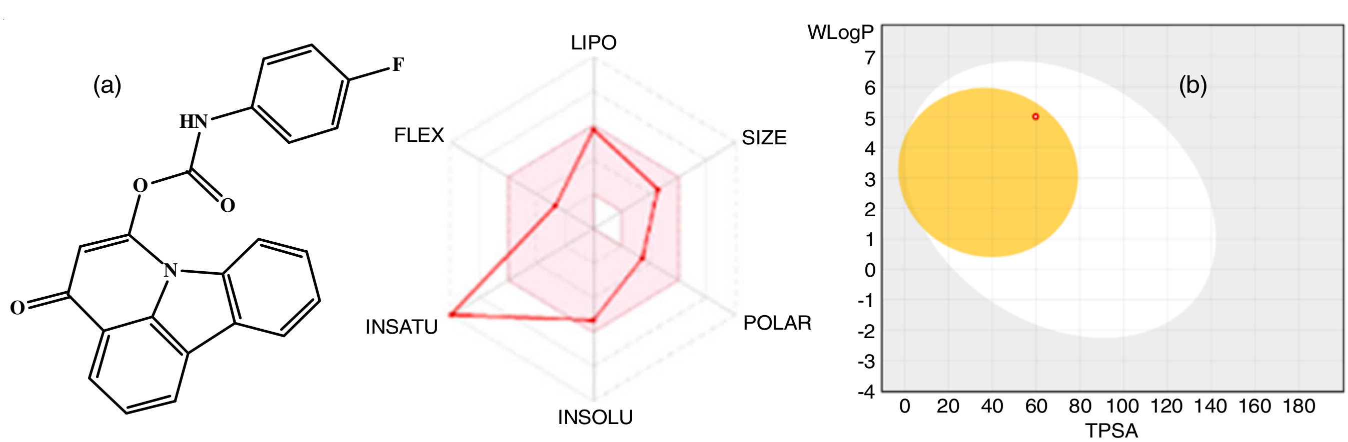

Fig. 6. ADME prediction (a) Radar plot and (b) Boiled egg model

tural binding phenomena of compound **4c** and also the ADME parameters of this molecule were also found to be in an acceptable range. It can thus be concluded that further optimization of the molecule can lead to the generation of more potent anti-Alzheimer's compounds.

ACKNOWLEDGEMENTS

The authors are thankful to Amity Institute of Pharmacy Lucknow for providing the necessary research facilities for the completion of this work.

CONFLICT OF INTEREST

The authors declare that there is no conflict of interests regarding the publication of this article.

REFERENCES

1. P. Scheltens, B. De Strooper, M Kivipelto, H. Holstege, G. Chételat, C.E. Teunissen, J. Cummings, W.M. van der Flier, *Lancet*, **397**, 1577 (2021); https://doi.org/10.1016/s0140-6736(20)32205-4
2. R.K. Chaudhary, U.V. Mateti, P. Khanal, K.B. Rawal, P. Jain, V.S. Patil, A.K. Shrivastava and B M Patil, Alzheimer's Disease: Epidemiology, Neuropathology and Neurochemistry, In: Computational and Experimental Studies in Alzheimer's Disease: CRC Press, pp. 1-14 (2024).
3. Alzheimer's Disease Facts and Figures, *Alzheimers Dement.*, **20**, 3708 (2024); https://doi.org/10.1002/alz.13809
4. S. Samanta, M. Ramesh and T. Govindaraju, in eds.: T. Govindaraju, Alzheimer's Disease: Recent Findings in Pathophysiology, Diagnostic and Therapeutic Modalities, The Royal Society of Chemistry, Chap. 1, p. 34 (2022).
5. Z.R. Chen, J.B. Huang, S.L. Yang and F.F. Hong, *Molecules*, **27**, 1816 (2022); https://doi.org/10.3390/molecules27061816
6. K. Sharma, *Mol. Med. Rep.*, 20, 1479 (2019); https://doi.org/10.3892/mmr.2019.10374
7. M.B. Colovic, D.Z. Krstic, T.D. Lazarevic-Pašti, A.M. Bond•ic and V. M. Vasic, *Curr Neuropharmacol*., **11**, 315 (2013); https://doi.org/10.2174/1570159x11311030006
8. M. Saxena and R. Dubey, *Curr. Top. Med. Chem*., **19**, 264 (2019); https://doi.org/10.2174/1568026619666190128125912
9. D.B. Barbosa, M.R. do Bomfim, T.A. de Oliveira, A.M. da Silva, A.G. Taranto, J.N. Cruz, P.B. de Carvalho, J.M. Campos, C.B.R. Santos and F.H.A. Leite, *Pharmaceuticals*, **16**, 1657 (2023); https://doi.org/10.3390/ph16121657
10. N. Kumar, P. Gupta and S. Bansal, *Lett. Drug Design Discov.*, **19**, 1049 (2022); https://doi.org/10.2174/1570180819666220314144219
11. B.C. Nandy, A. Gupta, A. Mittal and V. Vyas, *J. Biomed. Pharm. Res*., **3**, 42 (2014).
12. L.S. Tsutsumi, D. Gündisch and D. Sun, *Curr. Top. Med. Chem*., **16**, 1290 (2016); https://doi.org/10.2174/1568026615666150915112647
13. A Caruso, A. Barbarossa, A. Carocci, G. Salzano, M.S. Sinicropi and C. Saturnino, *Appl. Sci.*, **11**, 6192 (2021); https://doi.org/10.3390/app11136192
14. A. Caruso, J. Ceramella, D. Iacopetta, C. Saturnino, M.V. Mauro, R. Bruno, S. Aquaro and M.S. Sinicropi, *Molecules*, **24**, 1912 (2019); https://doi.org/10.3390/molecules2410191
15. S.O. Bachurin, E.V. Bovina and A.A. Ustyugov, *Med. Res. Rev*., **37**, 1186 (2017); https://doi.org/10.1002/med.21434
16. C. Chen, X. Wang, D. Xu, H. Zhang, H.-N. Chan, Z. Zhan, S. Jia, Q. Song, G. Song, H.-W. Li and M.S. Wong, *J. Mater. Chem. B*, **11**, 4865 (2023); https://doi.org/10.1039/D3TB00082F
17. D.V. Patel, N.R. Patel, A.M. Kanhed, D.M. Teli, K.B. Patel, P.D. Joshi, S.P. Patel, P.M. Gandhi, B.N. Chaudhary, N.K. Prajapati, K.V. Patel and M.R. Yadav, *Bioorg. Chem*., **101**, 103 (2020); https://doi.org/10.1016/j.bioorg.2020.103977
18. Y.P. Singh, N. Kumar, B. S. Chauhan, and P. Garg, *Drug Dev. Res*., **84**, 1624 (2023); https://doi.org/10.1002/ddr.22113
19. A. Rampa, S. Montanari, L. Pruccoli, M. Bartolini, F. Falchi, A. Feoli, A. Cavalli, F. Belluti, S. Gobbi, A. Tarozzi and A. Bisi, *Future Med. Chem.*, **9**, 749 (2017); https://doi.org/10.4155/fmc-2017-0029
20. U. Košak, N. Strašek, D. Knez, M. Jukic, S. •akelj , A. Zahirovic, A. Pišlar, X. Brazzolotto, F. Nachon, J. Kos and S. Gobe, *Eur. J. Med. Chem.*, **197**, 112282 (2020); https://doi.org/10.1016/j.ejmech.2020.112282
21. H. Zhang, Y. Wang, Y. Wang, X. Li, S. Wang and Z. Wang, *Eur. J. Med. Chem*., **240**, 114606 (2022); https://doi.org/10.1016/j.ejmech.2022.114606
22. M. Alipour M. Khoobi, A. Moradi, H. Nadri, F.H. Moghadam, S. Emami, Z. Hasanpour, A. Foroumadi and A. Shafiee. *Eur. J. Med. Chem*., **82**, 536 (2014); https://doi.org/10.1016/j.ejmech.2014.05.056
23. N. Mishra and D. Sasmal, *Bioorg. Med. Chem. Lett.,* **23**, 702 (2013); https://doi.org/10.1016/j.bmcl.2012.11.100
24. H. Akrami, B.F. Mirjalili, M. Khoobi, A. Moradi, A. Sakhteman, H. Nadri, S. Emami, A. Foroumadi and A. Shafiee, *Eur. J. Med. Chem.*, **84**, 375 (2014); https://doi.org/10.1016/j.ejmech.2014.01.017
25. E. Nepovimova, J. Korabecny, R. Dolezal, K. Babkova, A. Ondrejicek, D. Jun, V. Sepsova, A. Horova, M. Hrabinova, O. Soukup, N. Bukum, P. Jost, L. Muckova, J. Kassa, D. Malinak, M. Andrs and K. Kuca, *J. Med. Chem.*, **58**, 8985 (2015); https://doi.org/10.1021/acs.jmedchem.5b01325
26. S.P. Mantoani, T.P.C. Chierrito, A.F.L. Vilela, C.L. Cardoso, A. Martínez and I. Carvalho, *Molecules*, **21**, 193 (2016); https://doi.org/10.3390/molecules21020193
27. S.L. Motebennur, B.P. Nandeshwarappa and M.S. Katagi, *Drugs Drug Cand.*, **2**, 571 (2022); https://doi.org/10.3390/ddc2030030
28. Z.-M. Wang, P. Cai, Q.-H. Liu, D.-Q. Xu, X.-L. Yang, J.-J. Wu, L.-Y. Kong and X.-B. Wang, *Eur. J. Med. Chem*., **123**, 282 (2016); https://doi.org/10.1016/j.ejmech.2016.07.052
29. W. Stadlbauer, V.H. Dang and N. Guttenberger, *J. Heterocycl. Chem*., **52**, 114 (2014); https://doi.org/10.1002/jhet.1994
30. P. Bar-On, C.B. Millard, M. Harel, H. Dvir, A. Enz, J.L. Sussman and I. Silman, *Biochemistry*, **41**, 3555 (2002); https://doi.org/10.1021/bi020016x
31. A. Daina, O. Michielin and V. Zoete, *Sci. Rep*., **7**, 42717 (2017); https://doi.org/10.1038/srep42717
32. A. Daina and V. Zoete, *Chem. Med. Chem.*, **11**, 1117 (2016); https://doi.org/10.1002/cmdc.201600182
33. M. Pohanka, M. Hrabinova, K. Kuca and J.P. Simonato, *Int. J. Mol. Sci.*, **12**, 2631 (2011); https://doi.org/10.4149/BLL_2013_153
34. M. Shahrivar-Gargari, M. Hamzeh-Mivehroud, S. Hemmati, J.S. Mojarrad, T.T. Kuçukkilinç, B. Ayazgok and S. Dastmalchi, *Arch. Pharm*., **354**, 2000453 (2021); https://doi.org/10.1002/ardp.202000453